An integrative approach assesses the intraspecific variations of *Procamallanus* (*Spirocamallanus*) *inopinatus*, a common parasite in Neotropical freshwater fishes, and the phylogenetic patterns of Camallanidae

Lorena G. Ailán-Choke[1], Luiz E.R. Tavares[2], José L. Luque[3], Felipe B. Pereira[4*]

[1]Consejo Nacional de Investigaciones Científicas y Técnicas (CONICET), Instituto para el Estudio de la Biodiversidad de Invertebrados, Facultad de Ciencias Naturales, Universidad Nacional de Salta, Av. Bolivia 5150, (4400) Salta, Argentina.

[2]Departamento de Patologia, Instituto de Biociências, Universidade Federal de Mato Grosso do Sul, Av. Costa e Silva s/n°, CEP 79070-900, Campo Grande, MS, Brasil.

[3]Departamento de Parasitologia Animal, Instituto de Veterinária, Universidade Federal Rural do Rio de Janeiro, BR 465, Km 47, CEP 23851-970, Seropédica, RJ, Brasil.

[4]Departamento de Parasitologia, Instituto de Ciências Biológicas, Universidade Federal de Minas Gerais, Av. Presidente Antônio Carlos, 6627, Pampulha, CEP 31270-901, Belo Horizonte, MG, Brasil.

Runing Title: Integrative taxonomy of camallanids

[*]Corresponding author: Prof. Dr. Felipe Bisaggio Pereira

Address: Departamento de Parasitologia, Instituto de Ciências Biológicas, Universidade Federal de Minas Gerais, Av. Presidente Antônio Carlos, 6627, Pampulha, CEP 31270-901, Belo Horizonte, MG, Brasil.

Phone: +55 31 3409 3065

e-mail: felipebisaggiop@hotmail.com

This is an Accepted Manuscript for Parasitology. This version may be subject to change during the production process. DOI: 10.1017/S0031182020001687

Abstract

Integrative taxonomy was used to evaluate two component populations of *Procamallanus* (*S*pirocamallanus) *inopinatus* in Brazil and the phylogeny Camallanidae. Parasite populations were collected in the characiform *Anostomoides passionis* from River Xingu (Amazon basin) and *Megaleporinus elongatus* from River Miranda (Paraguay basin). Morphology was analysed using light and scanning electron microscopy (SEM). Genetic characterisation was based on partial sequences of the 18S and 28S rDNA, and COI mtDNA. Phylogenies were based on 18S and COI due to data availability. Generalized Mixed Yule Coalescent (GMYC), Poisson Tree Process (PTP) and *BEAST were used for species delimitation and validation. SEM revealed for the first time the presence of minute denticles and pore-like structures surrounding oral opening, phasmids in females and confirmed other important morphological aspects. Statistical comparison between the two component populations indicated morphometric variations especially among males. The different component population of *P.* (*S.*) *inopinatus* showed variable morphometry, but uniform morphology, and were validated as conspecific by the GMYC, PTP and *BEAST. Some camallanid sequences in GenBank have incorrect taxonomic labelling. Host, environment and geographic aspects seem to be related to some lineages within Camallanidae; however, their real phylogenetic meanings are still unclear.

Keywords: Anostomidae, Characiformes, endoparasite, helminth, integrative taxonomy, Nematoda, genetic characterisation, morphology.

Introduction

Procamallanus (*Spirocamallanus*) *inopinatus* Travassos, Artigas & Pereira, 1928 was originally described infecting the characiform fishes *Leporinus copelandii* Steindachner, 1855 and *Megaleporinus elongatus* (Valenciennes, 1850) from River Paraná Basin, Brazil (Travassos *et al.* 1928; Kohn and Fernandes, 1987). Since then, the species has been reported in several families of Characiformes, Perciformes and Siluriformes, within a wide geographical range in South America including, besides Brazil, Argentina, Paraguay, Peru and Venezuela (see Moravec, 1998; Iannacone *et al*. 2000; Chemes and Takemoto, 2011; Luque *et al.* 2011, 2016).

Due to its common occurrence, the general morphology of *P*. (*S*.) *inopinatus* has been well investigated suggesting that the species has homogenous morphology, but quite variable morphometry among component populations (Petter and Dlouhy, 1985; Kohn and Fernandes, 1987; Petter and Thatcher, 1988; Moravec *et al.* 1993, 1997). Scanning electron microscopy (SEM) also has been used for observing the ultrastructure of *P*. (*S*.) *inopinatus*, but the detailing level was somewhat limited by the technology available at the time of such studies were performed (Moreira *et al.* 1994; Moravec *et al.* 1997). More recently, Vicentin *et al.* (2013) investigated *P*. (*S*.) *inopinatus* using SEM, but the approach of the study was not focused on the taxonomy of the species; therefore results were not detailed.

Due to the lack of genetic data for *P*. (*S*.) *inopinatus*, its phylogenetic position within Camallanidae is unknown and the discussions regarding its wide morphometric variations among different populations remain without this important subsidy. Indeed, the phylogenetic aspects of Camallanidae are far from being elucidated due to the lack of genetic data, which is aggravated by the fact that the morphology-based systematics of the family is problematic and taxonomic labelling of some sequences available in

genetic databases (e.g. GenBank) seems to be inaccurate (Černotíková *et al.* 2011; Sardella *et al.* 2017; Ailán-Choke *et al.* 2019).

Therefore, the present study aimed to compare component populations of *P.* (*S.*) *inopinatus* from two different host species and localities using an integrative taxonomic approach and evaluate the phylogenetic aspects of Camallanidae based on different computational tools (e.g. digital imaging, biostatistics, phylogenetic and species delimitation).

Materials and Methods

Sampling and processing of hosts and nematodes

Hosts were sampled as follows: 10 specimens of *Anostomoides passionis* Santos & Zuanon, 2006 (Characiformes: Anostomidae) from River Xingu (RX), municipality of Altamira, State of Pará, Brazil (3°14′S; 52°06′W) in April 2013, and 12 specimens of *M. elongatus* (Anostomidae) from River Miranda (RM), municipality of Corumbá, State of Mato Grosso do Sul, Brazil (19°28′S, 57°02′W) in August 2018. Fish were kept alive in small water tanks with oxygen pumps until necropsy, through a ventral longitudinal incision from anus to operculum and extraction of the digestive tract. Organs (oesophagus, stomach, caeca, intestine) were placed individually in Petri dishes with saline and analysed using a stereomicroscope.

Nematodes were found alive, washed in saline, fixed in hot 4% formaldehyde solution and preserved in 70% ethanol. For morphological observations, nematodes were cleared in glycerine. One male of each infrapopulation (i.e. from each infected fish, see also Bush *et al.* 1997 for details) had the mid body excised and fixed in molecular-grade 96–99% ethanol for genetic studies; anterior and posterior parts were fixed for morphological identification.

Nomenclature and classification of hosts were updated following Froese and Pauly (2019), Frost (2020) and Uetz *et al.* (2020).

Morphological procedures

Nematodes were cleared in glycerine and observed in a Leica DM5500 B microscope, with DIC and the software LAS Leica™, for morphometric analysis. Measurements are given in micrometres, unless otherwise stated. Specimens used for SEM (1 male and 1 female of each infrapopulation) were dehydrated through a graded ethanol series, dried by evaporation with hexamethyldisilazane, coated with gold and observed in a JEOL JSM 6460-LV, at an accelerating voltage of 15 kV. The systematic classification of camallanid nematodes follows the proposal of Moravec and Thatcher (1997). Voucher specimens were deposited in the Coleção Helmintológica do Instituto Oswaldo Cruz (accession nos. CHIOC 38939, 38940).

Statistical analysis of morphological data

In order to evaluate significant differences among morphometric features, we performed a series of statistical analyses. First, one sample Kolmogorov-Smirnov (K-S) test was performed to verify the normal distribution of the quantitative variables (Zar, 2010). The quantitative variables were the standard length (SL) of fishes, and total body length, maximum width, buccal capsule length and width, distance from anterior end to nerve ring, deirids and excretory pore, total length of oesophagus, tail length, distance from cephalic end to vulva in females and spicules in males of parasites. All these measurements were also used for calculating their ratio to total body length; the coefficient of variation (CV) for each of the previous mentioned features was also calculated. These morphometric features were chosen because they are used in the

specific diagnosis, and ratios were used for verifying if the organ's anatomy (or their locations on the cuticle surface) undergoes modifications according to the parasite growth. Ratios and CV are expressed in percentage (%) and mean values are followed by ± 1 standard deviation, unless otherwise stated.

According to the results of K-S test, we performed non-parametric inferential methods and generalised linear models (GLM). As a preliminary analysis, in order to verify possible influences of host-environment attributes and infection burden on the parasite body length, host SL and parasite intensity of infection (see Bush *et al.* 1997) were tested as predictive of parasite body length using linear regression (Zar, 2010). First, host SL and parasite intensity of infection were tested separately against parasite body length using simple linear regression, in order to evaluate which variable was most predictive through the r^2 (coefficient of determination). Then a multiple linear regression was performed, inserting the predictive variables into the expected predictive model, in which the most predictive was inserted first followed by the less predictive (Zar, 2010). Following the previous methodology, but using logistic regression instead of linear, we tested the effect of host species and parasite sexual maturation (i.e. male, non-gravid and gravid females) on parasite body length, estimating the odds ratio (OR, $0 < OR < 1$ indicates antagonistic effect; $OR = 1$ lack of effect; $OR > 1$ synergetic effect) and the confidence interval (CI) of each model (Dohoo *et al.* 2003). We also performed a Mann-Whitney (U) to evaluate and prove the differences in SL among the two fish species (Zar, 2010).

Following the preliminary analysis, parasites were divided into three categories according to sexual maturation: males, non-gravid females (without larvae in uterus) and gravid females (uterus filled with larvae). All morphometric features previously stated for parasites were tested against their total body length using the Spearman's

correlation (r_s) (Zar, 2010), considering all sexual maturation categories. Differences in morphometric features of parasites among the two component populations, i.e. from *A. passionis* and *M. elongatus*, were evaluated using the *U* test, within each sexual maturation category and among non-gravid and gravid females (Zar, 2010). Additional terminology related to parasite ecology follows the proposal of Bush *et al.* (1997).

Genetic procedures

Genomic DNA was isolated using DNeasy Blood & Tissue Kit (QIAGEN, Hilden, Germany), following the manufacturer's instructions. Three genetic regions were amplified: the 5' end of the 18S nuclear rDNA, the D2 and D3 domains of the nuclear 28S rDNA and the COI of the mtDNA. All PCR reactions, cycling conditions and primers are detailed in Supplementary Material 1. PCR products were purified through an enzymatic treatment with ExoProStar™ (GE Helathcare) and sent for sequencing at ACTGene (Ludwig Biotec, Rio Grande do Sul, Brazil) with the same primers used in PCR reactions.

Contiguous sequences were assembled in Geneious (Geneious ver. 9.1.5 created by Biomatters, available from http://www.geneious.com/) and deposited in the GenBank. Preliminary BLAST search on GenBank database (https://www.ncbi.nlm.nih.gov/genbank/) was performed to confirm the genetic proximity between the present sequences and those from representatives of Camallanidae.

Phylogenetic analyses of molecular data

The phylogenetic reconstructions were based on three different datasets: with sequences of the 18S rDNA, with those of COI mtDNA and with sequences of 18S and COI

concatenated. Due to the small number of sequences of the 28S rDNA and the high frequency of genetic gaps after aligning them, phylogenies based on this genetic region were not reconstructed; we used this genetic marker only for comparisons between the present samples. Sequences were chosen according to the following criteria: genetic regions congruent with those obtained in the present study and minimum length of 744 bp and 355 bp for 18S and COI, respectively (for details see Table 1). Sequences from samples not identified to species level and clones were excluded. We tried to use as much representatives as possible, including different samples from a same species for species delimitation and validation analyses. The outgroup was chosen according to previous phylogenies of Camallanidae (see Černotíková *et al.* 2011). Sequences were aligned using M-Cofee (Notredame *et al.* 2000), then evaluated by the transitive consistency score, to verify the reliability of aligned positions and, based on score values, ambiguous aligned positions were trimmed (Chang *et al.* 2014). Saturation of nucleotide substitution was tested using Xia's method implemented in DAMBE (Xia *et al*. 2003; Xia, 2018).

Datasets were subjected to maximum likelihood (ML) and Bayesian inference (BI) analyses, using PHYML and MrBayes, respectively (Huelsenbeck and Ronquist, 2001; Guindon and Gascuel, 2003). The model of evolution (nucleotide substitution) and its fixed parameters for each dataset were chosen and estimated under the Akaike information criterion with jModelTest 2 (Guindon and Gascuel, 2003; Darriba *et al.* 2012); in the dataset of 18S + COI the partitions were treated separately and substitution models unlinked (see details in Supplementary Material 2). Nodal supports for ML were based on 1,000 bootstrap non-parametric replications. The same, but for BI posterior probability, were determined after running the Markov chain Monte Carlo (MCMC) (2 runs 4 chains) for 4×10^6 generations, with sampling frequency every 4×10^3

generations and discarding the initial ¼ of sampled trees (1×10^6) as bur-in. In order to check chain convergence, analyses were run in duplicates and inspected using Tracer (Rambaut *et al.* 2018).

The genetic markers profile of phylogenetic informativeness was evaluated by PhyDesign (Townsend, 2007) based on the concatenated dataset (18S + COI). For this analysis, an ultrametric tree was generated using BEAST 2.5 (Bouckaert *et al.* 2019), the best-fit substitution model was chosen according to bModelTest (Bouckaert and Drummond, 2017), models of each partition were unlinked, clock model was selected based on marginal likelihood estimated (MLE) from stepping stone and path sampling (Baele *et al.* 2012) being 50 path steps, 5×10^5 itinerations and sampling every 500 generations. MCMC chains were run for 5×10^7 generations, sampling every 5×10^3 generations and ¼ of initial runs discarded as burn-in. All analyses were run in duplicates and inspected with Tracer to check convergence. More information can be found in Supplementary Material 2.

Species delimitation

We tested species hypotheses within Camallanidae mainly focused on the present samples. Two different species discovery methods and one species validation method were used to delimit species boundaries. Some analyses required ultrametric trees; these were generated in BEAST 2.5 as previously described and additional details are also in Supplementary Material 2.

For species discovery we used the Generalized Mixed Yule Coalescent (GMYC) method and the Poisson Tree Process (PTP) method, which do not require a priori assignments regarding putative species (Pons *et al.* 2006; Zhang *et al.* 2013). The GMYC requires an ultrametric guide tree, uses ML to delimit species and estimates a

transition point before which all nodes reflects species diversification events and after which all nodes represent population-coalescent process (Pons *et al.* 2006; Razkin *et al.* 2016). GMYC tests were run in the web server (http://species.h-its.org/gmyc) under the single-threshold and multiple-threshold models, for each dataset. The PTP does not require ultrametric trees; therefore, the major consensus tree generated from BI of each dataset, were used in the analysis; this method try to identify significant changes in the rate branching of the phylogenetic tree, using number of substitutions. These analyses were run in the bPTP web server (http://species.h-its.org/ptp) using the default settings (1×10^5 generations, thinning set to 100, burn-in 1×10^4), which are adequate for datasets with < 50 taxa according to Zhang *et al.* (2013). PTP run both ML and BI to support the delimited species.

To validate the species, we used *BEAST (Heled and Drummond, 2010) implemented in BEAST 2.5 to generate unrooted (in order to improve species delimitation results; see Zhang *et al.* 2013) species trees based on each dataset (minus outgroup sequences). *BEAST uses BI approach to generate phylogenies. We considered samples from a same species as different populations, since they are mostly originating from different host individuals (see Table 1). Substitution models were chosen based on bModelTest, molecular clock selected based on MLE from stepping stone and path sampling, Yule process species tree priors and a constant root population size model. MCMC chains were run for 1×10^8 generations, sampling every 2×10^3 generations and ¼ of initial runs discarded as burn-in. Chains were run in duplicates and inspected with Tracer to check convergence. More information can be found in Supplementary Material 2.

We also used the Automatic Barcode Gap Discovery (ABGD) method (Puillandre *et al.* 2012) to generate pairwise (patristic) distance (*P*) matrixes, and thus

evaluate intra and interspecific divergences among samples according to each genetic marker. The ABGD analyses were run online (http://wwwabi.snv.jussieu.fr/public/abgd/) using Kimura two-parameter (K2P) (Kimura, 1980) as distance metric, with other parameters set to default. We refrain from account the partitions generated by ABGD, since intraspecific divergence of 18S and COI are poorly known and editing ABGD parameters for intraspecific genetic distance would generate mistaken results.

Results

The prevalence of *P*. (*S*.) *inopinatus* found in the present study was 30% (3 parasitized/10 examined) in *A*. *passionis* and 25% (3/12) in *M*. *elongatus*. The mean intensity of infection was 7.3 ± 1.5 (ranging from 6–9 parasites per infected host) in *A*. *passionis* and 8.0 ± 2.6 (0–11 per analysed host) in *M*. *elongatus*. Therefore, there were two component populations (one from each host/locality) each composed of three infrapopulations of the parasite. *Procamallanus* (*S*.) *inopinatus* component population in *A*. *passionis* from RX had 9 males, 6 non-gravid and 7 gravid females; that in *M*. *elongatus* form RM had 11 males, 5 non-gravid and 8 gravid females. No concurrent infections were observed (i.e. the only helminth found was *P*. (*S*.) *inopinatus*). Specimens of *M*. *elongatus* were larger (SL 35.4 ± 1.3 cm; range 34.5–37.3 cm) than those of *A*. *passionis* (23.9 ± 1.2 cm; 23–25.5 cm); this difference was statistically significant ($p < 0.001$). The GLMs indicated no significant effect of host species ($p > 0.78$), SL ($p > 0.37$) and parasite intensity of infection ($p > 0.59$) in parasite body length. However, there was significant effect in parasite body length by sexual maturation ($p < 0.001$), in which males predicted smaller body length (OR = 0.687; CI

0.599–0.721), non-gravid females intermediate body length (OR = 1.233; CI 1.014–2.357) and gravid females larger body lengths (OR = 3.542; CI 2.987–3.881).

The following diagnostic features were constant and observed in the present specimens using SEM: cephalic end with two median teeth (one dorsal and one ventral) (Fig. 1A, B, Supplementary Material 3), males with 10 pairs of subventral and sessile caudal papillae (4 pairs pre and 6 pairs prostcloacal) (Fig. 1E, F) and females without distinct terminal appendix on tail (Fig. 1G, H). Also based on SEM observations, the presence of 6 pore-like structures (2 subdorsal, 2 subventral and 2 lateral) and of small pointed denticles surrounding the oral opening (Fig. 1A–D), as well as the phasmids of females (Figs. 1G, H) are reported for the first time. The morphometric variations of the present specimens were within the range reported in previous studies. For these comparative measurements, as well as information on host and locality of these studies see Supplementary Material 4.

Most morphometric features of the present parasite specimens showed CV < 15%, with exception of some measurements related to deirids, excretory pore, tail and distance from anterior end to vulva in females (see Supplementary Material 5). The only CV higher than 20%, were observed in the ratio of excretory pore to total body length (CV = 26.3%) and in the distance of vulva from anterior end (CV = 24.3%), in gravid females from *A. passionis* (Supplementary Material 4). Most morphometric features were correlated with total body length of the parasites showing moderate to strong association (r^2 ranging from |0.594| to |0.928|), except by the length of tail (p = 0.07), length of spicules (p = 0.6), distance of vulva form anterior end (p = 0.9) and its relative position (p = 0.1) in females (Supplementary Material 5). The size of all anatomic structures (except those previously mentioned) showed positive correlation with total body length; conversely their ratios to total body length were negatively correlated, with

exception of that of spicule (Supplementary Material 5). Gravid females were larger and wider than those non gravid (both $p < 0.001$), the tail to body length ratio was higher in non-gravid ($p < 0.001$) and vulva was more posterior in gravid specimens ($p = 0.01$); however, the relative position of vulva was similar in both gravid and non-gravid females ($p = 0.2$) (Table 2, Supplementary Material 5). Width of buccal capsule and length of oesophagus were also higher in gravid females ($p = 0.014$ and < 0.001, respectively); distance from anterior end to deirid and nerve ring to total body length ratio also showed statistical differences according to female ontogeny (Table 2, Supplementary Material 5).

Comparing the two component populations of *P*. (*S*.) *inopinatus*, based on morphometry and according to sex and female ontogeny, most statistical divergences were observed among males. All measurements tended to be higher in males parasitizing *A*. *passionis*; however, the significance comparing the body length was in the borderline (i.e., $p = 0.05$) and the significant differences were found in buccal capsule length ($p = 0.003$) and width ($p = 0.006$), in excretory pore location ($p = 0.03$), as well as in the length of oesophagus ($p = 0.003$), spicules ($p < 0.03$) and tail ($p = 0.003$) (Table 2, Supplementary Material 4). No statistical differences were observed comparing the morphometry of gravid females from *A*. *passionis* and *M*. *elongatus*, and regarding the non-gravid specimens from *A*. *passionis* showed wider buccal capsule ($p = 0.01$), more posterior excretory pore ($p = 0.03$) and larger oesophagus ($p = 0.01$) (Table 2, Supplementary Material 5).

After sequencing of the genetic regions, 18S (GenBank accession nos. MT901634; MT901635) and COI (MT898796; MT898796) showed no polymorphisms within samples of the same component population; therefore we used only one representative of each component population for genetic analyses. Three different

genotypes were found for the 28S (MT901636–MT901638), two from parasites of *A. passionis* and one from *M. elongatus*, in which the genetic similarity among then was > 98% (sequence lengths were 870 bp, 874 bp and 876 bp).

The partial 18S fragments were 892 bp long and showed only one polymorphism in the position 640 (A/C) according to component populations; their genetic similarity was 99.89% and the patristic distance $P = 0.00116$. *Promacallanus* (*S.*) *pintoi* (Kohn & Fernandes, 1988) in the freshwater catfish *Corydoras atropersonatus* Weitzman & Nijssen, 1970 from Peru (DQ442666), was most similar to the present samples (genetic of similarity 94.13% and $P = 0.0117$ when compared with those parasites of *M. elongtus*; genetic similarity of 94.24% and $P = 0.0105$ when compared with those parasites of *A. passionis*). The partial coding fragments of COI were 388 bp long, the genetic similarity among samples from *M. elongtus* and *A. passionis* was 90.72%, the patristic distance $P = 0.09901$ and no polymorphism resulted in amino acid residue change. These sequences were most similar to that of *P.* (*S.*) *istiblenni* (Noble, 1966) parasitizing the marine snapper *Lutjanus kasmira* (Forsskål, 1775) from Hawaii (KC517382) (genetic similarity 86.18% and $P = 0.1515$ from parasites of *M. elongtus* and 84.75% and $P = 0.1700$ from parasites of *A. passionis*). Genetic alignments showed no substantial nucleotide saturation (18S: Iss = 0.068, Iss.c = 0.804, $p < 0.001$; COI: Iss = 0.2612, Iss.c = 0.6761, $p < 0.001$). BLAST search indicated that the representative from GenBank database most genetic similar to the present sequences was *C. xenopodis* Jackson & Tinsley, 1995 [MG947389] (genetic similarity of 64.4%).

The phylogenies using 18S sequences included more representative taxa than those using COI and 18S + COI, because data availability (Table 1, Figs 2–4). The phylogenetic meaning of the trees reconstructed using ML and BI was the same; therefore, only BI trees were depicted. Monophyly of Camallanidae was strongly

supported in all phylogenies (Figs. 2, 3); in contrast, its genera and subgenera were not monophyletic (Figs. 2, 4). A monophyletic assemblage including sequences with the same origin from India, shaded in the trees of the 18S, made the following species not monophyletic: *Camallanus cotti* Fujita, 1927, *C. oxycephalus* Ward & Magarth, 1917 and *P.* (*S.*) *istiblenni*. *Procamallanus* (*S.*) *rarus* Travassos, Artigas & Pereira, 1935 was also non-monophyletic and unrelated to the shaded clade (Figs. 2, 4). Samples from the present study formed well-supported monophyletic assemblages in all the phylogenies (Figs. 2–4). The phylogenetic informativennes of COI was better for analysing divergences and similarities among inner nodes (e.g. closely related taxa, such as those species) and that of 18S better for evaluating divergence events related to more external nodes (e.g., for comparing genera) (Fig. 3).

Regarding the species delimitation analyses, PTP was more concordant with the molecular phylogenetic approach than GMYC (Figs. 2, 3). ML of the GMYC was significantly higher than the null model, except for the 18S dataset (see Supplementary Material 6). The entities recognised by the PTP model showed high support values for both ML and Bayesian approaches (see Supplementary Material 6). The present samples were recognised as a single species by both methods, in all datasets (Figs. 2, 3). In the tree of 18S sequences, PTP indicated that *P.* (*S.*) *istiblenni* represented 7 different specific entities, *C. oxycephalus* 6, *C. cotti* and *P.* (*S.*) *rarus* 2 each (Fig. 2). In the tree of COI sequences, PTP agreed with taxonomic labelling of all species, except *B. slomei* and *B. xenopodis* that were recognised as a single species (Fig. 2), and the K2P distance between these sequences (MG948463/ MN523681) was null ($P = 0$). The concordance of these methods (mainly PTP) with the taxonomic labelling of the sequences was higher in the dataset of COI and 18S + COI sequences, as expected (Figs. 2, 3).

Species tree approach validated the results of phylogenetic and species delimitation methods (mainly of PTP) (Figs. 2–4). Samples of *P*. (*S*.) *inopinatus* were validated as a single species, whereas those that appeared as non-monophyletic were not validated as single species, and, as same as in species delimitation approach, *B*. *slomei* and *B*. *xenopodis* and recognised as a single lineage; nodal supports in these cases were medium to high (Fig. 4). We indicated host, geographic origin and environmental features related to samples in the species tree of 18S and COI (Fig. 4). Thus, most phylogenetic assemblages did not show similarities regarding these characteristics, except the clade A in Fig. 4 that grouped species from freshwater hosts and the shaded one, composed of species from India, with no additional information. These clades showed average nodal supports (Fig. 4). It should be mentioned that *P*. (*S*.) *inopinatus* was phylogenetically close to samples isolated from freshwater fishes of the Neotropical region.

The pairwise distances between samples of *P*. (*S*.) *inopinatus* were $P = 0.001$ and $P = 0.099$ in 18S and COI matrices, respectively. Lower than these, were the distances between representative of *P*. (*S*.) *fulvidraconis* Li, 1935 (DQ076689/JF803914) and *P*. (*S*.) *istiblenni* (EF180076/KC505629) (both $P = 0$) in 18S matrix, representatives of *C*. *cotti* (DQ442662/EU598876/EU598845; $P < 0.014$) , *C*. *oxycephalus* (EU598879/EU598876/EU598833/EU598845; $P < 0.014$) of *P*. (*S*.) *istiblenni* (KC517382/KC517383; $P = 0.002$) and between *B*. *slomei* Southwell & Krishner, 1937 (MG948463) and *B*. *xenopodis* (MN523681) ($P = 0$) in COI matrix. Pairwise distances also corroborated previous phylogenetic, species delimitation and validation results, in which representatives of *C*. *cotti*, *C*. *oxycephalus* and *P*. (*S*.) *istiblenni* forming the shaded clade (Figs. 2, 4) showed values of genetic distance relatively high ($P > 0.013$) when compared with their conspecifics placed out of this

clade. Samples of *P.* (*S.*) *rarus* (DQ494195/JF803912) also showed similar results (*P* = 0.048). Complete distance matrices and comparative tables are available in Supplementary Material 7, 8, 9.

Discussion

As previously commented, *Procamallanus* (*S.*) *inopinatus* is a nematode parasite with suggestively low host specificity and wide distribution in the freshwaters of South America (from North to South-western Brazil, Venezuela, Peru and Argentina) (see Moravec, 1998; Chemes and Takemoto, 2011; Luque *et al.* 2011, 2016). Some aspects of its taxonomic assessment have been controversial, especially considering the spiral ridges in buccal capsule (see Moravec *et al.* 1993, 1997). Despite the wide variation in the number of spiral ridges in *P.* (*S.*) *inopinatus* (13–23, see Supplementary Material 4), they occupied no more than 2/3 of the buccal capsule as shown herein and in other studies (Travassos, 1928; Pereira, 1935; Kloss, 1966; Petter and Thatcher, 1988; Moravec *et al.* 1993, 1997; Abdalla *et al.* 2012). Reciprocally, Petter and Dlouhy (1985) described this structure completely occupied by the spiral ridges and Vicentin *et al.* (2013) reported the same characteristic, but based only on female specimens; both studies analysed characiform fishes from River Paraguay basin (as in the present study). These observations indicate that this characteristic may be a rare intraspecific variation in *P.* (*S.*) *inopinatus*. However, to confirm this assertion, specimens with the whole buccal capsule occupied by spiral ridges need to be genetically characterised and compared to the present data. It should be mentioned that, based on genetic evidence, the morphology of buccal capsule seems to bears some degree of artificiality in the

systematics of genera and subgenera of Camallanidae (Wijová *et al*. 2006; Sardella *et al*. 2017; Ailán-Choke *et al*. 2019), which may be also true at species level, as suggested here.

Moreira *et al.* (1994) performed the first observation of *P*. (*S*.) *inopinatus* using SEM and reported 3 circles of 4 cephalic papillae each in the species. Later, Moravec *et. al.* (1997) described only 2 circles with 4 papillae each, also using SEM. Base on the present results it was possible to confirm the observations of Moreira *et al.* (1994) through higher resolution micrographs. The present observations also reported for the first time small denticles and pore-like structures surrounding the oral opening internally and externally, respectively. It should be mentioned that Vicentin *et al.* (2013) reported only 1 circle of 4 cephalic papillae in *P*. (*S*.) *inopinatus*, which is a misinterpretation since in the SEM micrograph provided by the authors it is possible to observe the 2 additional circles of cephalic papillae (see Fig. 1A by Vicentin *et al.* 2013). The presence of two large (dorsal and ventral) teeth (see Moravec and Thatcher, 1988; Moreira *et al*. 1994) were also confirmed and phasmids in female observed for the first time, contributing to the morphological knowledge of *P*. (*S*.) *inopinatus*.

The present results showed that almost all measurements used for taxonomic diagnosis had medium to strong correlation with the body length of parasites. Measurements of the organs showed a positive correlation (except the length of spicules and the distance from cephalic and to vulva) whereas the ratio of these measurements to total body length showed negative correlation (see Supplementary Material 5). It indicates that the growth rates of body and organs are markedly different, in which the first grows much faster than the second (a matter of mathematic reason: if the divisor, i.e., body length, is much higher than the dividend, i.e., measure of a given organ, the quotient will be low). Moreover, these results indicate general morphometric

dependence on body length, except by the spicule length and the relative position of vulva, which are more constant and, consequently, more reliable for intraspecific comparisons, regardless of body length and sexual maturation of *P*. (*S*.) *inopinatus*.

Sexual maturation of females of *P*. (*S*.) *inopinatus* in the present study had significant effect on their body length, in which gravid specimens were larger than the non-gravid. As a consequence, some ratio measurements, the maximum body and buccal capsule width, oesophagus length, distance from cephalic end to vulva, but not its relative position (vulva to body length ratio), were statistically different (Table 2, Supplementary Material 5). Therefore, the morphometry of gravid and non-gravid females should be presented separately. However, several studies do not follow this proposal, making the morphometric range of females of *P*. (*S*.) *inopinatus* very wide (see Supplementary Material 4). Male specimens are evidently smaller than females (present results showed males as predictive of smaller body length), and also exhibit the same wide morphometric ranges, comparing the present results with the previous studies (see Supplementary Material 4). Thus, researches should be aware when dealing with the morphometry of *P*. (*S*.) *inopinatus* and focus on morphology (see further discussion).

Despite intensity of infection, host species and SL did not have an effect in the body length of the present parasites; the statistical comparison between specimens of the two component populations evidenced the morphometric differences from males and non-gravid females, but not from those gravid. It indicates that, once these females reach full sexual maturity, their growth stabilizes (other argument supporting the assertion for separating measurements from non-gravid and gravid specimens). The main differences comparing non-gravid females and males from the two component populations were in the position of excretory pore and in the length of oesophagus;

these variations can be observed in *P*. (*S*.) *inopinatus* from different hosts and river basins (Petter and Dlouhy, 1985; Petter and Thatcher, 1988; Moravec *et al.* 1993, 1997). Although the body length is similar between males from the present component populations, specimens parasitizing *A*. *passionis* showed larger spicules. The size of these structures is very important in the taxonomy of *Procamallanus* (*Spirocamallanus*) spp. (Moravec *et al*. 2000; Moravec and Jirků, 2015; Pinheiro *et al*. 2018; Moravec and Justine, 2019). However, in *P*. (*S*.) *inopinatus* the length of spicules seems to be random and not correlated with body length, some of the smallest males have average spicule length (e.g. Petter and Thatcher, 1988) whereas some of the larger specimens have them short (e.g. Moravec *et al.* 1997) (see also Supplementary Material 4).

The present morphometric heterogeneity observed in *P*. (*S*.) *inopinatus* represents a phenotypic plasticity characteristic of the species, also observed in previous studies (see Supplementary Material 4). Moreover, although the morphology of *P*. (*S*.) *inopinatus* is almost constant, the number and distribution of spiral ridges on its buccal capsule is highly variable. In fact, these features have been pointed out as weak taxonomic characters within the complicated systematics of Camallanidae (Wijová *et al.* 2006; Černotíková *et al.* 2011; Sardella *et al.* 2017; Ailán-Choke *et al*. 2019). Therefore, in order to avoid further taxonomic confusions, we suggest that the specific diagnosis of *P*. (*S*.) *inopinatus* should be based on the presence of two large (one dorsal and one ventral) oral teeth at the cephalic end, which represent the single autapomorphy of the species so far.

The present and first genetic characterisation of *P*. (*S*.) *inopinatus* supported the results of morphological analysis, in which the morphology of the specimens was constant among the component populations. It also reaffirms the characteristic wide morphometric variation of the species. The pairwise distances of both 18S and COI

among the present sequences were low, as same as observed between representatives of *C. cotti* (DQ442662/EF180071 from 18S and EU598833/ EU598845 EU598876/EU598879 from COI), *P.* (*S.*) *istiblenni* (KC505629/ KC505630 from 18S and KC517382/ KC517383) and *P.* (*S.*) *fulvidraconis* (DQ076689/ JF803914 from 18S) (for more details see Supplementary Material 7, 8). The present 28S sequences also supported that the samples are conspecific; their genetic similarity was much higher than that of the most closely related sample form GenBank database (i.e. *C. xenopodis*). Unfortunately, 28S sequences from GenBank are currently very limited in number and length, giving no robustness for comparing the present intraspecific genetic variations with that from other species. Similarly, species delimitation and validation approaches indicated that *P.* (*S.*) *inopinatus* in *A. passionis* from River Xingu (Amazon basin) and in *M. elongatus* from River Miranda (Paraguay basin) are conspecific. It should be highlighted that GMYC was more conservative than PTP, regarding species delimitation, and the accuracy of the methods was higher in the databases including COI (see Supplementary Material 6), because this genetic region was more informative for analysing divergences and similarities among closely related taxa than the 18S (see Fig. 3); this is due to the fact that, in metazoans, mtDNA genes evolve at faster rates than those form nuclear DNA (Allio *et al*. 2017).

The overall phylogeny of Camallanidae was poorly resolved and monophyly was not observed in most genera and subgenera as a consequence of the morphology-based systematics that predominantly uses the buccal capsule structure as diagnostic feature, which seems to be artificial as commented previously (Wijová *et al.* 2006; Černotíková *et al.* 2011; Sardella *et al.* 2017; Ailán-Choke *et al*. 2019).

The genus *Batrachocamallanus* Jackson & Tinsley, 1995 is a particular case; it has been considered synonym of *Procamallanus* (*Procamallanus*) Baylis, 1923 by some

authors (Moravec *et al.* 2006) and valid by others (Jackson and Tinsley, 1995; Svitin *et al.* 2018, 2019). The buccal capsule structure in both taxa is the same and the characters used in the differential diagnosis of *Batrachocamallanus* were refuted and proved to be also present in *Procamallanus* (*Procamallanus*) (see Moravec *et al*. 2006). Therefore, we agree with the proposal of Moravec *et al.* (2006) and consider *Batrachocamallanus* junior synonym of *Procamallanus* (*Procamallanus*). In this sense, the present genetic analyses support the previous assertion because GMYC considered the two representatives, labelled *B*. *slomei* Southwell & Kirshner, 1937 and *B*. *xenopodis* (Baylis, 1929), along with *P*. (*P*.) *spiculocubernaculus* Agarwal, 1958 as a single species and in the species tree they were closely related with full nodal support. Furthermore, sequences from *B*. *slomei* and *B*. *xenopodis* were 100% similar, but we will not assume their synonymy, since data represents only a small and partial fragment of a gene.

In the phylogenetic reconstructions using 18S sequences, representatives of *P*. (*S*.) *inopinatus* formed a fully supported assemblage with *P*. (*S*.) *pintoi*, which was also closely related to *P*. (*S*.) *rarus* and *P*. (*S*.) *huacraensis* Ramallo, 2008, all representatives isolated from freshwater catfishes, in the Amazon (the first two) and la Plata basin (the last). When COI sequences were included in the analysis, the phylogenetic position of *P*. (*S*.) *inopinatus* was somewhat uncertain, but not in the species tree that provides better genealogy of taxa (Nichols, 2001) and where it formed a fully supported assemblage with *P*. (*S*.) *huacraensis*. The recent ancestrally of the all previously mentioned species is probably the same (or closely related), since the geological and biogeographic history in South America, indicates the close relatedness between the Amazon la and Plata basins (which includes Paraná basin), and the tandem evolution of their fish fauna (Albert and Reis, 2011; Reis *et al.* 2016; Dagosta and

Pinna, 2017). Moreover, *P*. (*S*.) *inopinatus* also parasitizes catfishes (see Moravec, 1998; Iannacone *et al*. 2000; Chemes and Takemoto, 2011; Luque *et al.* 2011, 2016). These relationships between habitat, host taxa, geographic origin and the phylogenetic aspects of camallanids cannot be generalised and are unclear, since as same as some assemblages were formed by samples isolated from freshwater hosts, they were from very different geographic origins and host taxa; other assemblages were formed independent from these characteristics. Similar results were previously observed (Wijová *et al.* 2006; Ailán-Choke *et al.* 2019).

The conspecific-labelled sequences referring to *C*. *cotti*, *C*. *oxycephalus*, *P*. (*S*.) *istiblenni* and *P*. (*S*.) *rarus* were not monophyletic. The main responsible for this result was the shaded clade in Figs 2, 4, composed by sequences with the same origin (location and authors), with poorly detailed information and unpublished in scientific papers. The usage of these sequences generated misleading results, which were kept here with the intent of highlighting the importance of a careful analysis when dealing with the genetic database of camallanids, since these data have considerable taxonomic inaccuracies also observed in other studies (Černotíková *et al.* 2011; Ailán-Choke *et al*. 2019).

The present approach confirmed that the general morphometry of *P*. (*S*.) *inopinatus* is markedly variable, whereas the general morphological features are constant, especially the following that should be used for species diagnosis: the presence of two large (dorsal and ventral) oral teeth (only synapomorphy of the species), the relative position of vulva (on the second third of body) and 10 then pairs of subventral caudal papillae in males (4 pairs pre and 6 pair post cloacal). The present genetic characterisation and the phylogenetic analyses supported the morphological analyses and that the component populations of *P*. (*S*.) *inopinatus* from *A*. *passionis* and

M. elongatus are conspecific, their genetic structure differ, but this difference is minimal regarding all genetic markers analysed. The data provided here improves the current scarce genetic database of camallanid nematodes and represents the first step for a better understanding of the genetic population structure of *P.* (*S.*) *inopinatus*.

Acknowledgements

The authors would like to thank Dr. Elias Nogueira de Aguiar from the Laboratório Multiusuário de Análises de Materiais do Instituto de Física (MULTILAM-INFI), Universidade Federal de Mato Grosso do Sul (UFMS), for help with scanning electron microscopical procedures. Dr. Carina Elisei from the Universidade Católica Dom Bosco provided the facilities for molecular studies. Dr. Philippe Vieira Alves for valuable conversations that inspired the approach of the present manuscript and Lennon de Souza Malta for his assistance in field collections and laboratorial procedures.

Ethical Standards

All procedures involving animal manipulation were permitted by Sistema de Informação e Autorização em Biodiversidade (license number 54895) and were in strict accordance with the recommendations of the Colégio Brasileiro de Experimentação Animal.

Financial Support

This work was financed in part by the Coordenação de Aperfeiçoamento de Pessoal de Nível Superior-Brasil (CAPES)-Finance code 001 and by the Conselho Nacional de Desenvolvimento Científico e Tecnológico – Brazil (Proc. 474077/2011-0).

Conflict of interest

None.

References

Abdallah, V.D., Azevedo, R.K., Carvalho, E.D. and Silva, R.J. (2012). New hosts and distribution records for nematode parasites of freshwater fishes from São Paulo State, Brazil. *Neotropical Helminthology* **6**, 43–57.

Ailán-Choke, L.G., Davies, D.A., Tavares, L.E.R. and Pereira, F.B. (2019). An integrative taxonomic assessment of *Procamallanus* (*Spirocamallanus*) *huacraensis* (Nematoda: Camallanidae), infecting the freshwater catfish Trichomycterus spegazzinii (Siluriformes: Trichomycteridae) in Argentina. *Parasitology Research* **118**, 2819–2829. https://doi.org/10.1007/s00436-019-06429-0

Albert, J.S. and Reis, R.E. (2011). *Historical Biogeography of Neotropical Freshwater Fishes*. Berkeley, CA: University of California Press.

Allio, R., Donega, S., Galtier, N. and Nabholz B. (2017). Large variation in the ratio of mitochondrial to nuclear rate across animals: implications for genetic diversity and the use of mitochondrial DNA as a molecular marker. *Molecular Biology and Evolution* **34**, 2762–2772. https://doi.org/10.1093/molbev/msx197

Baele, G., Li, W.S., Drummond A.J., Suchard, M.A. and Lemey, P. (2012). Accurate Model Selection of Relaxed Molecular Clocks in Bayesian Phylogenetics. Molecular *Biology and Evolution* **30**, 239–243. https://doi.org/10.1093/molbev/mss243

Bouckaert, R. and Drummond, A. (2017). bModelTest: Bayesian phylogenetic site model averaging and model comparison. *BMC Evolutionary Biology* **17**, 42. https://doi.org/10.1186/s12862-017-0890-6

Bouckaert, R., Vaughan, T.G., Barido-Sottani, J., Duchêne, S., Fourment, M., Gavryushkina, A., Heled, J., Jones, G., Kühnert, D., De Maio, N., Matschiner, M., Mendes, F.K., Müller, N.F., Ogilvie, H.A., du Plessis, L., Popinga, A., Rambaut, A., Rasmussen, D., Siveroni, I., Suchard, M.A., Wu, C-H., Xie, D., Zhang, C., Stadler,

T. and Drummond, A.J. (2019). BEAST 2.5: An advanced software platform for Bayesian evolutionary analysis. *PLoS Computational Biology* **15**, e1006650. https://doi.org/10.1371/journal.pcbi.1006650

Bush, A.O., Lafferty, K.D., Lotz, J.M. and Shostak, A.W. (1997). Parasitology meets ecology on its own terms: Margolis et al. revisited. *Journal of Parasitology* **83**, 575–583. https://doi.org/10.2307/3284227

Černotíková, E., Horák, A. and Moravec, F. (2011). Phylogenetic relationships of some spirurine nematodes (Nematoda: Chromadorea: Rhabditida: Spirurina) parasitic in fishes inferred from SSU rRNA gene sequences. *Folia Parasitologica* **58**, 135–148. https://doi.org/10.14411/fp.2011.013

Chang, J-M., Di Tommaso, P. and Notredame, C. (2014). TCS: A new multiple sequence alignment reliability measure to estimate alignment accuracy and improve phylogenetic tree reconstruction. *Molecular Biology and Evolution* **31**, 1625–1637. https://doi.org/10.1093/molbev/msu117

Chemes, S.B. and Takemoto, R.M. (2011). Diversity of parasites from middle Paraná system freshwater fishes, Argentina. *International Journal of. Biodiversity and Conservation* **3**, 249–266.

Dagosta, F.C.P. and Pinna, M. (2017). Biogeography of Amazonian fishes: deconstructing river basins as biogeographic units. *Neotropical Ichthyology* **15**, e170034. https://dx.doi.org/10.1590/1982-0224-20170034

Darriba, D., Taboada, G.L., Doallo, R. and Posada, D. (2012). jModelTest 2: more models, new heuristics and parallel computing. *Nature Methods* **9**, 772. https://doi.org/10.1038/nmeth

Dohoo, I., Martin, W. and Stryhn, H. (2003). *Veterinary Epidemiologic Research*. AVC Inc., Charlottetown.

Froese, R. and Pauly, D. (Eds) (2019). FishBase. World Wide Web electronic publication. http//www.fishbase.org (accessed 25 May 2020).

Frost, D.R. (2020). Amphibian Species of the World: an Online Reference. Version 6.1. World Wide Web electronic publication. https://amphibiansoftheworld.amnh.org/index.php. (accessed 25 august 2020). doi.org/10.5531/db.vz.0001

Guindon, S. and Gascuel, O. (2003). A simple, fast, and accurate algorithm to estimate large phylogenies by maximum likelihood. *Systematic Biology* **52**, 696–704. http://doi.org/10.1080/10635150390235520

Heled, J. and Drummond, A.J. (2010). Bayesian inference of species trees from multilocus data, *Molecular Biology and Evolution* **27**, 570–580. https://doi.org/10.1093/molbev/msp274

Horton, T. *et al.* (2020). World Register of Marine Species. World Wide Web electronic publication. https://www.marinespecies.org (accessed 25 august 2020). https://doi.org/10.14284/170

Huelsenbeck, J.P., Ronquist, F. (2001). MrBayes: Bayesian inference of phylogenetic trees. *Bioinformatics* **17**, 754–755. https://doi.org/10.1093/bioinformatics/17.8.754

Iannacone, J.A., López, E.N. and Alvariño, L.F. (2000). *Procamallanus* (*Spirocamallanus*) *inopinatus* Travassos, Artigas et Pereira, 1928 (Nematoda: Camallanidae) parásito de *Triportheus angulatus* (Spix, 1829) (Characidae) en la laguna de Yarinacocha, Ucayali-Peru. *Biologia Pesquera* **28**, 37–43.

Jackson, J.A. and Tinsle, R.C. (1995). Representatives of *Batrachocamallanus* n. g. (Nematoda: Procamallaninae) from *Xenopus* spp. (Anura: Pipidae): geographical distribution, host range and evolutionary relationships. *Systematic Parasitology* **31**, 159–188. https://doi.org/10.1007/BF00009115

Kimura, M. (1980). A simple method for estimating evolutionary rates of base substitutions through comparative studies of nucleotide sequences. *Journal of Molecular Evolution* **16**, 111–120.

Kloss, G.R. (1966). Helmintos parasitos de espécies simpátricas de *Astyanax* (Pisces, Characidae). *Papéis Avulsos do Departamento de Zoologia* São Paulo **18**, 189–219.

Kohn, A. and Fernandes, B.M.M. (1987). Estudo comparativo dos helmintos parasitos de peixes do Rio Mogi Guassu, coletados nas excursões realizadas entre 1927 e 1985. *Memórias do Instituto Oswaldo Cruz* **82**, 483–500.

Luque, J.L., Aguiar, J.C., Vieira, F.M., Gibson, D.I. and Portes-Santos, C. (2011). Checklist of Nematoda associated with the fishes of Brazil. *Zootaxa* **3082**, 1–88.

Luque, J.L., Cruces, C., Chero, J., Paschoal, F., Alves, P.V., Da Silva, A.C., Sanchez, L. and Iannacone, J. (2016). Checklist of metazoan parasites of fishes from Peru. *Check List* **6**, 659–667.

Moravec, F. (1998). *Nematodes of Freshwater Fishes of the Neotropical Region*. Praha, Academia.

Moravec, F. and Justine, J.-L. (2019). A new species and new records of camallanid nematodes (Nematoda, Camallanidae) from marine fishes and seas snakes in New Caledonia. *Parasite* **26**, 66. https://doi.org/10.1051/parasite/2019068

Moravec, F., Justine, J.-L., Würtz, J., Tarachewski, H. and Sasal, P. (2006). A new species of *Procamallanus* (Nematoda: Camallanidae) from Pacific eels (*Anguilla* spp.). *Journal of Parasitology* **92**, 130–137. https://doi.org/10.1645/GE-3509.1

Moravec, F. and Jirků, M. (2015). Two *Procamallanus* (*Spirocamallanus*) species (Nematoda: Camallanidae) from freshwater fishes in Lower Congo River. *Acta Parasitologica* **60**, 226–233. https://doi.org/10.1515/ap-2015-0032

Moravec, F., Kohn, A. and Fernandes, B.M.M. (1993). Nematode parasites of fishes of the Paraná River, Brazil. Part 3. Camallanoidea and Dracunculoidea. *Folia Parasitologica* **40**, 211–229.

Moravec, F., Prouza, A. and Royero, R. (1997). Some nematodes of freshwater fishes in Venezuela. *Folia Parasitologica* **44**, 33–47.

Moravec, F., Salgado-Maldonado, G. and Caspeta-Mandujano, J. (2000). Three new *Procamallanus* (*Spirocamallanus*) species from freshwater fishes in Mexico. *Journal of Parasitology* **86**, 119 –127. https://doi.org/10.1645/0022-3395(2000)086[0119:TNPSSF]2.0.CO;2

Moravec, F. and Thatcher, V.E. (1997). *Procamallanus* (*Denticamallanus* subgen. n.) *dentatus* sp. n. (Nematoda, Camallanidae) from the characid fish, *Bryconops alburnoides*, in the Brazilian Amazon. *Parasite* **4**, 239–243.

Moreira, N.I.B., Oliveira, C.L. and Costa, H.M.A. (1994). *Spirocamallanus inopinatus* (Travassos, Artigas & Pereira, 1928) e *Spirocamallanus saofranciscencis* sp. n. (Nematoda, Camallanidae) em peixes da Represa de Tres Maria. *Arquivo Brasileiro de Medicina Veterinária e Zootecnia* **46**, 485–500.

Notredame, C., Higgins, D.G. and Heringa, J. (2000). T-Coffee: A novel method for fast and accurate multiple sequence alignment. *Journal of Molecular Biology* **302**, 205–217. https://doi.org/10.1006/jmbi.2000.4042

Pereira, C. (1935). Ascaridata e Spirurata parasitos de peixes do Nordeste Brasileiro. *Arquivos do Instituto Biológico São Paulo* **6**, 53–62.

Petter, A.J. (1974). Deux nouvelles especes de Nématodes Camallanina parasites de *Hoplerythrinus unitaeniatus* (Characidae, Cypriniformes) en Guyane; création d´ une nouvelle famille: les Guyanemidae (Dracunculoidea). *Bulletin du Museum National d'Histoire Naturelle* **156**, 803–812.

Petter, A.J. and Dlouhy, C. (1985). Nématodes de Poissons du Paraguay. III. Camallanina. Description d'une espèce et d'une sous-espèce nouvelles de la famille des Guyanemidae. *Revue Suisse de Zoologie* **92**, 165–175.

Petter, A.J. and Thatcher, V.E. (1988). Observations sur la structure de la capsule buccale de *Spirocamallanus inopinatus* (Nematoda), parasite de poissons brésiliens. *Bulletin du Museum National d'Histoire Naturelle* **10**, 685–692.

Pinheiro, R.H. da S., Melo, F.T.V., Monks, S., dos Santos, J. N. and Giese, E.G. (2018). A new species of *Procamallanus* Baylis, 1923 (Nematoda, Camallanidae) from *Astronotus ocellatus* (Agassiz, 1831) (Perciformes, Cichlidae) in Brazil. *Zookeys* **790**, 21–33. https://doi.org/10.3897/zookeys.790.24745

Pons, J., Barraclough, T.G., Gomez-Zurita, J., Cardoso, A., Duran, D.P., Hazell, S., Kamoun, S., Sumlin, W.D. and Vogler, A.P. (2006). Sequence-based species delimitation for the DNA taxonomy of undescribed insects. *Systematic Biology* **55**, 595–609. https://doi.org/10.1080/10635150600852011

Puillandre, N., Lambert, A., Brouillet, S. and Achaz, G. (2012). ABGD, Automatic Barcode Gap Discovery for primary species delimitation. *Molecular Ecology* **21**, 1864–1877. https://doi.org/10.1111/j.1365-294X.2011.05239.x

Rambaut, A., Drummond, A.J., Xie, D., Baele, G. and Suchard, M.A. (2018). Posterior summarization in Bayesian phylogenetics using Tracer 1.7. *Systematic Biology* **67**, 901–904. https://doi.org/10.1093/sysbio/syy032

Razkin, O., Sonet, G., Breugelmans, K., Madeira, M.J., Gómez-Moliner, B.J. and Backeljau, T. (2016). Species limits, interspecific hybridization and phylogeny in the cryptic land snail complex Pyramidula: the power of RADseq data. *Molecular Phylogenetics and Evolution* **101**, 267–278. https://doi.org/10.1016/j.ympev.2016.05.002

Reis, R.E., Albert, J.S., Di Dario, F., Mincarones, M.M., Petry, P. and Rocha, L.A. (2016). Fish biodiversity and conservation in South America. *Journal of Fish Biology* **89**, 12–47. https://doi.org/10.1111/jfb.13016

Sardella, C.J., Pereira, F.B. and Luque, J.L. (2017). Redescription and first genetic characterisation of *Procamallanus* (*Spirocamallanus*) *macaensis* Vicente & Santos, 1972 (Nematoda: Camallanidae), including re-evaluation of the species of *Procamallanus* (*Spirocamallanus*) from marine fishes off Brazil. *Systematic Parasitology* **94**, 657–668. https://doi.org/10.1007/s11230-017-9728-2

Svitin, R., Schoeman, A.L. and du Preez L.H. (2018). New information on morphology and molecular data of camallanid nematodes parasitising *Xenopus laevis* (Anura: Pipidae) in South Africa *Folia Parasitologica* **65**, 003. https://doi.org/10.14411/fp.2018.003

Svitin, R., Truter, M., Kudlai, O., Smit, N.J. and du Preez L. (2019). Novel information on the morphology, phylogeny and distribution of camallanid nematodes from marine and freshwater hosts in South Africa, including the description of *Camallanus sodwanaensis* n. sp. *International Journal for Parasitology: Parasites and Wildlife* **10**, 263–273. https://doi.org/10.1016/j.ijppaw.2019.09.007

Townsend, J.P. (2007). Profiling phylogenetic informativeness. *Systematic Biology* **56**, 222–231. https://doi.org/10.1080/10635150701311362.

Travassos, L., Artigas, P. and Pereira, C. (1928). Fauna helmintológica dos peixes de água doce do Brasil. *Arquivos do Instituto Biológico* **1**, 5–68.

Uetz, P., Freed, P. and Hosek, J. (Eds) (2020). The Reptile Database. World Wide Web electronic publication. http://www.reptile-database.org (accessed 25 May 2020)

Vicentin, W., Vieira, K.R.I., Tavares, L.E.R., Costa, F.E., Takemoto, R.M. and Paiva, F. (2013). Metazoan endoparasites of *Pygocentrus nattereri* (Characiformes:

Serrasalminae) in the Negro River, Pantanal, Brazil. *Revista Brasileira de Parasitologia Veterinária* **22**, 331–338. https://doi.org/10.1590/S1984-29612013000300003

Wijová, M., Moravec, F., Horák, A. and Lukeš, J. (2006). Evolutionary relationships of Spirurina (Nematoda: Chromadorea: Rhabditida) with special emphasis on dracunculoid nematodes inferred from SSU rRNA gene sequences. *International Journal for Parasitology* **36**, 1067–1075. https://doi.org/10.1016/j.ijpara.2006.04.005

Xia, X. (2018). DAMBE 7: New and improved tools for data analysis in molecular biology and evolution. *Molecular Biology and Evolution* **35**, 1550–1552. https://doi.org/10.1093/molbev/msy073

Xia, X., Xie, Z. and Li, W.H. (2003). Effects of GC content and mutational pressure on the lengths of exons and coding sequences. *Journal of Molecular Evolution* **56**, 362–370. https://doi.org/10.1007/s00239-002-2406-1

Zar, J.H. (2010). *Biostatistical Analysis*. Prentice Hall, Englewood Cliffs.

Zhang, J., Kapli, P., Pavlidis, P. and Stamatakis, A. (2013). A general species delimitation method with applications to phylogenetic placements. *Bioinformatics* **29**, 2869–2876. https://doi.org/10.1093/bioinformatics/btt499

Table 1. Species whose sequences were obtained from GenBank and used in phylogenetic reconstructions, associated with their hosts (habitat: Freshwater [FW] or Marine [MA]), geographic origin, accession number and genetic regions. The 18S refers to the rRNA gene and the COI to the cytochrome c oxidase subunit I mtDNA. Superscript numbers make correspondence between information.

Parasite species	Host (habitat)	Geographic origin	18S	COI
Batrachocamallanus slomei[*]	*Xenopus laevis* (FW)	South Africa	–	MG948463
Batrachocamallanus xenopodis	*Xenopus muelleri* (FW)	South Africa	–	MN523681
Camallanus cotti	*Lentipes concolor* (FW)[1]; *Awaous guamensis* (FW)[2]; *Opsariichthys bidens* (FW)[3]; *Odontobutis obscurus* (FW)[4]	New Caledonia[2]; China[3, 4]; India[5]	EF180071[1]; DQ442662[2]; GU082507[5]	EU598879[3]; EU598876[4]; EU598845[4]; EU598833[4];
Camallanus hypophthalmichthys	*Aristichthys nobilis* (FW)[1]	China[1]	JF803915[1]	EU598816
Camallanus kaapstaadi	*Xenopus laevis* (FW)	South Africa	–	MG948461
Camallanus lacustris	*Sander lucioperca* (FW)	Czech Republic	DQ442663	–
Camallanus oxycephalus	*Lepomis* sp. (FW)[1]	India[2]	DQ503463[1]; GU082496[2]; GU082497[2]; GU170847[2]; GU170848[2]; GU170849[2];	–
Camallanus xenopodis	*Xenopus laevis* (FW)	South Africa	–	MG948462
Paracamallanus cyathopharynx	*Clarias gariepinus* (FW)	South Africa	–	MN523683
Procamallanus (*P.*) *annulatus*	*Siganus lineatus* (MAR)	New Caledonia	JF803932	–
Procamallanus (*P.*) *laeviconchus*	*Synodontis schall* (FW)	Sudan	JF803934	–
Procamallanus (*P.*) *pacificus*	*Anguilla obscura* (FW)	New Caledonia	DQ442665	–

Procamallanus (*P.*) *pseudolaeviconchus*	*Clarias gariepinus* (FW)	South Africa	–	MN523682
Procamallanus (*P.*) *sigani*	*Siganus fuscescens* (MAR)	China	HM545908	–
Procamallanus (*P.*) *spiculogubernaculus*	*Heteropneustes fossilis* (FW)	India	KU292357	KU292358
Procamallanus (*S.*) *fulvidraconis*	*Pelteobagrus fulvidraco* (FW)[1, 2]	China[1,2]	JF803914[1]; DQ076689[2]	–
Procamallanus (*S.*) *huacraensis*	*Trichomycterus spegazzinii* (FW)	Argentina	MK794615	MK780067
Procamallanus (*S.*) *istiblenni*	*Lutjanus fulvus* (MAR)[1]; *Lutjanus kasmira* (MAR)[2]	Hawaii[2]; India[3]	EF180076[1]; KC505629[2]; KC505630[2]; GU082491[3]; GU082492[3]; GU082493[3]; GU082495[3]; GU170858[3]	KC517382[2]; KC517383[2]
Procamallanus (*S.*) *macaensis*	*Paralonchurus brasiliensis* (MAR)	Brazil	KY436826	–
Procamallanus (*S.*) *monotaxis*	*Lethrinus genivittatus* (MAR)	New Caledonia	JF803931	–
Procamallanus (*S.*) *philippinensis***	*Siganus guttatus* (MAR)	Philippines	JF934736	–
Procamallanus (*S.*) *pintoi*	*Corydoras atropersonatus* (FW)	Peru	DQ442666	–
Procamallanus (*S.*) *rarus*	*Aguarunichthys* cf. *tocantinsensis* (FW)[1]; *Callophysus macropterus* (FW)[2]	Peru[1, 2]	DQ494195[1]; JF803912[2]	–
Procamallanus (*S.*) *rebecae*	*Cichlasoma meeki* (FW)	Mexico	DQ442667	–
Serpinema cayennensis	*Rhinoclemmys punctularia* (FW)	French Guiana	–	MN104841
*Spirocerca lupi****	–	–	AY751497	MH633995

*Referred as *Procamallanus slomei* in GenBank; **Considered taxon inquirendum according to Horton *et al*. 2020; ***Used as outgroup.

Table 2. Comparative measurements of *Procamallanus* (*Spirocamallanus*) *inopinatus* in the present study, according to host and locality. Different superscript letters indicate measurements that showed statistical differences based on Mann-Whitney test, these comparisons are within each line of the table, respecting sexual maturation (more information see Supplementary Material 5).

Host	*Anostomoides passionis*			*Megaleporinus elongatus*		
Locality	River Xingu			River Miranda		
Specimens	Male (n = 9)	Gravid female (n = 7)	Non-gravid female (n = 6)	Male (n = 11)	Gravid female (n = 8)	Non-gravid female (n = 5)
Body length (mm)	6.87–7.57[a]	20.38–31.00[b]	15.25–18.32[c]	5.23–7.78[a]	20.57–24.37[b]	15.32–21.84[c]
Maximum width	351–361[a]	572–826[b]	396–501[c]	150–240[a]	680–760[b]	400–615[c]
Buccal capsule ridges[*]	13	13–15	13	11–14	17	12–16
Buccal capsule length	95–104[a]	113–127[c]	117–122[c]	68–91[b]	113–142[c]	119–137[c]
Buccal capsule width	76–112[a]	123–146[c]	132–134[d]	70–78[b]	123–158[c]	110–122[e]
Muscular oesophagus length[*]	404–451	409–578	449–501	270–370	500–550	350–400
Glandular oesophagus length[*]	598–646	821–1,170	770–855	410–550	925–940	510–745
Muscular/glandular oesophagus length ratio (%)[*]	63–70	46–55	57–65	54–73	53–54	51–78
Total oesophagus length (mm)	1–1.1[a]	1.23–1.75[c]	1.23–1.34[d]	0.71–0.92[b]	1.43–1.44[c]	0.91–1.13[e]
Total oesophagus/body length ratio (%)	15.8–17.4[a]	5.00–7.20[c]	7.70–9.70[c, d]	10.3–13.7[b]	5.08–5.90[c]	5.20–6.80[c, e]
Nerve ring to anterior end	174–210[a]	251–286[b]	253–262[b]	121–208[a]	235–270[b]	215–280[b]

This is an Accepted Manuscript for Parasitology. This version may be subject to change during the production process. DOI: 10.1017/S0031182020001687

Nerve ring to anterior end/body length ratio (%)	2.5–3.0[a]	0.8–1.2[b]	1.4–1.7[c]	1.7–3.1[a]	0.9–1.0[b]	1.1–1.7[c]
Deirids to anterior end	113–145[a]	136–158[b]	141–146[b]	107–130[a]	140–252[b]	139–145[b]
Deirids to anterior end/body length ratio (%)	1.6–1.9[a]	0.5–0.7[b]	0.8–0.9[c]	1.6–2.1[a]	0.6–1.0[b]	0.6–0.9[c]
Excretory pore to anterior end	310–430[a]	368–485[c]	387–476[c, d]	182–260[b]	340–390[c]	280–400[c, e]
Excretory pore to anterior end/body length ratio (%)	4.4–5.6[a]	1.1–2.3[c]	2.0–3.0[c, d]	2.6–4.1[b]	1.4–1.6[c]	1.3–2.4[c, d]
Spicule length	126–145[a]	–	–	90–132[b]	–	–
Spicule/body length ratio (%)	1.9–2.0[a]	–	–	1.3–2.0[b]	–	–
Vulva to anterior end (mm)	–	11.89–17.20[a]	8.00–9.36[b]	–	11.30–13.93[a]	8.41–12.04[b]
Relative position of vulva (%)	–	53.0–58.3[a]	51.0–55.0[a]	–	46.3–56.7[a]	52.4–64.7[a]
Tail length	291–322[a]	180–200[a]	180–187[a]	168–268[b]	180–210[a]	160–280[a]
Tail/body length ratio (%)	4.2–4.4[a]	0.6–0.9[c]	1.0–1.2[d]	2.4–4.1[b]	0.6–0.9[c]	0.9–1.2[d]

*Measurements not included in the statistical analysis.

Figure Legends

Fig. 1. *Procamallanus* (*Spirocamallanus*) *inopinatus*, ex. *Anostomoides passionis* (A, C, G, H) and *Megaleporinus elongates* (B, D, E, F), SEM micrographs **A, B:** Cephalic end of female and male, respectively, apical view (dashed lines delimit oral teeth). **C, D:** Oral opening of female and male, respectively (arrowheads indicate pore-like structures). **E, F:** posterior end and tail of male, respectively, sublateral views. **G, H:** tail and posterior end of female, respectively, sublateral views.

Fig. 2. Phylogenetic trees generated using Bayesian Inference from sequences of camallanid nematodes. Nodal supports are indicated on tree nodes, according to the Bayesian posterior probability (BPP) and maximum likelihood (ML) bootstrap replications as follows: full squares (BPP = 1, ML = 100%), full circles (0.96 < BPP < 1, 90% < ML < 100%) and empty circles (0.90 < BPP < 0.96, 95% < ML < 90%). Black polygons next to taxa labels indicate specific entities recognised by the Poisson Tree Process (PTP) and those white by the Generalized Mixed Yule Coalescent (GMYC); superscript numbers make correspondence with information in Table 1. The shaded clade represents atypical phylogenetic behaviour and includes sequences with apparently taxonomic misidentification. Sequences from de present study are in bold and superscriptions are RM = River Miranda, RX = River Xingu.

Fig. 3. Phylogenetic trees generated from concatenated sequences of the 18S rDNA and COI mtDNA of camallanid nematodes using Bayesian Inference. Upper centre tree is output of Mr. Bayes (gene tree), bottom right is output of PhyDesign (which does not estimates nodal supports) associated with graphical representation of phylogenetic informativeness for each generic marker, bottom left is a species tree output of *BEAST from 18S and COI concatenated. Nodal supports are indicated on tree nodes, according

This is an Accepted Manuscript for Parasitology. This version may be subject to change during the production process. DOI: 10.1017/S0031182020001687

to the Bayesian posterior probability (BPP) and maximum likelihood (ML) bootstrap replications as follows: full squares (BPP = 1, ML = 100%), full circles (0.96 < BPP < 1, 90% < ML < 100%) and empty circles (0.90 < BPP < 0.96, 95% < ML < 90%). Black polygons next to taxa labels indicate specific entities recognised by the Poisson Tree Process (PTP) and those white by the Generalized Mixed Yule Coalescent (GMYC); superscript numbers make correspondence with information in Table 1. Sequences from de present study are in bold and superscriptions are RM = River Miranda, RX = River Xingu.

Fig. 4. Species trees based on 18S rDNA and COI mtDNA sequences of camallanid nematodes generated using *BEAST, for species validation. Nodal supports are indicated on tree nodes, according to the Bayesian posterior probability (BPP) as follows: full squares (BPP = 1), full circles (0.96 < BPP < 1) and empty circles (0.90 < BPP < 0.96). Superscript numbers make correspondence with information in Table 1. The shaded clade represents atypical phylogenetic behaviour and includes sequences with apparently taxonomic misidentification. Letter A highlights the clade formed exclusively by species from freshwater hosts. Order of hosts, geographic origin and environment associated with each sequence are depicted. Sequences from de present study are in bold and superscriptions are RM = River Miranda, RX = River Xingu.

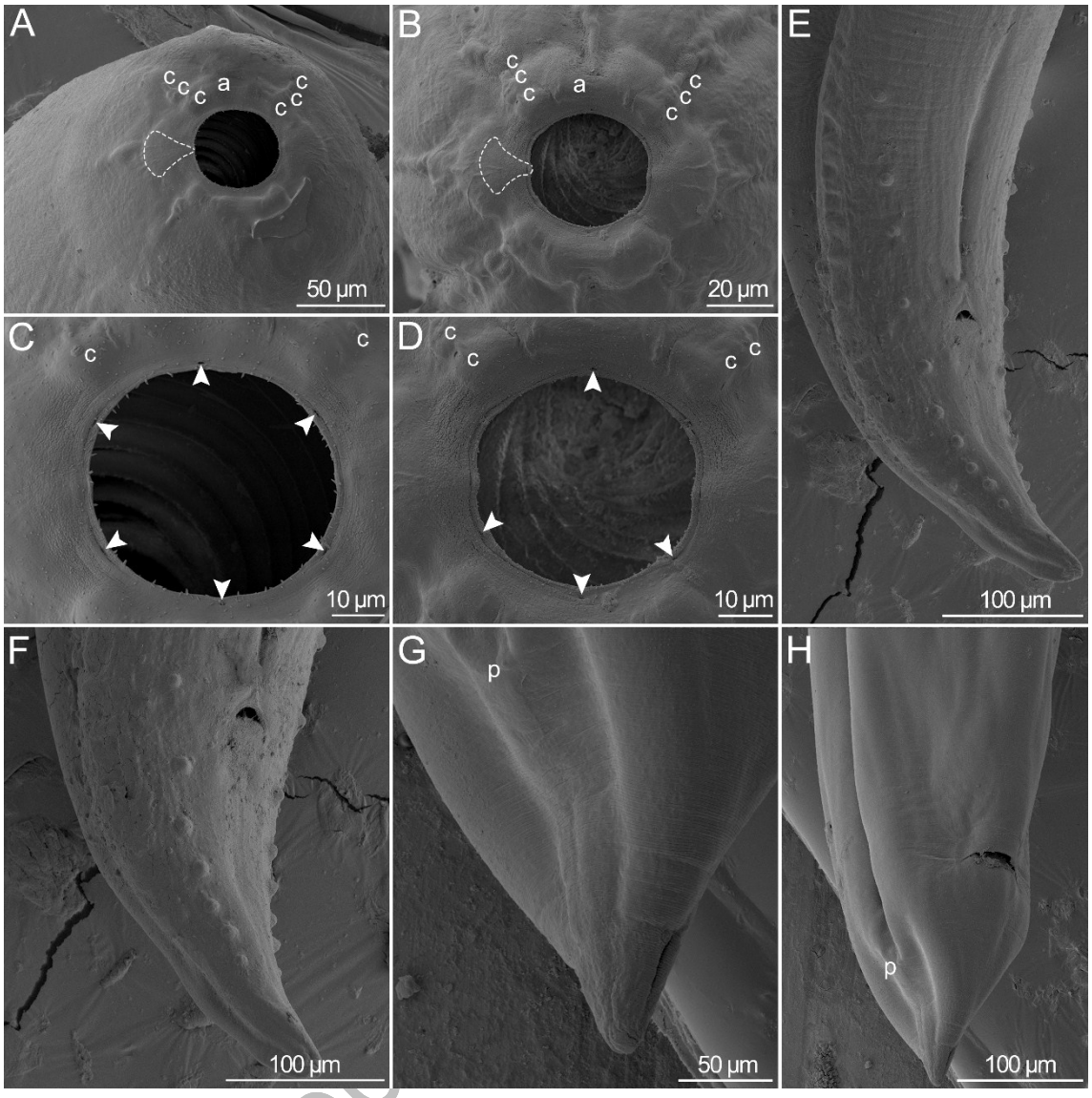

Figure 1.

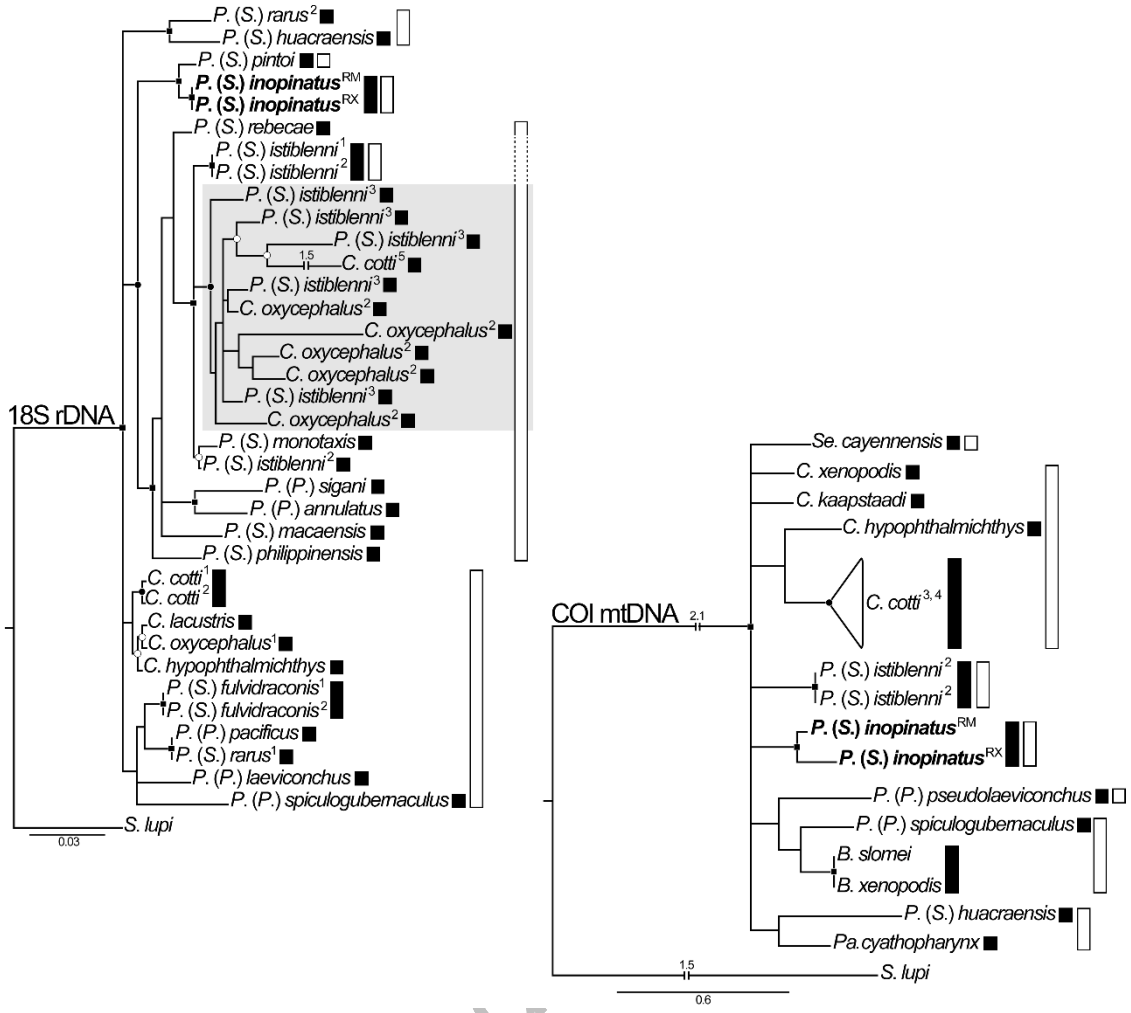

Figure 2.

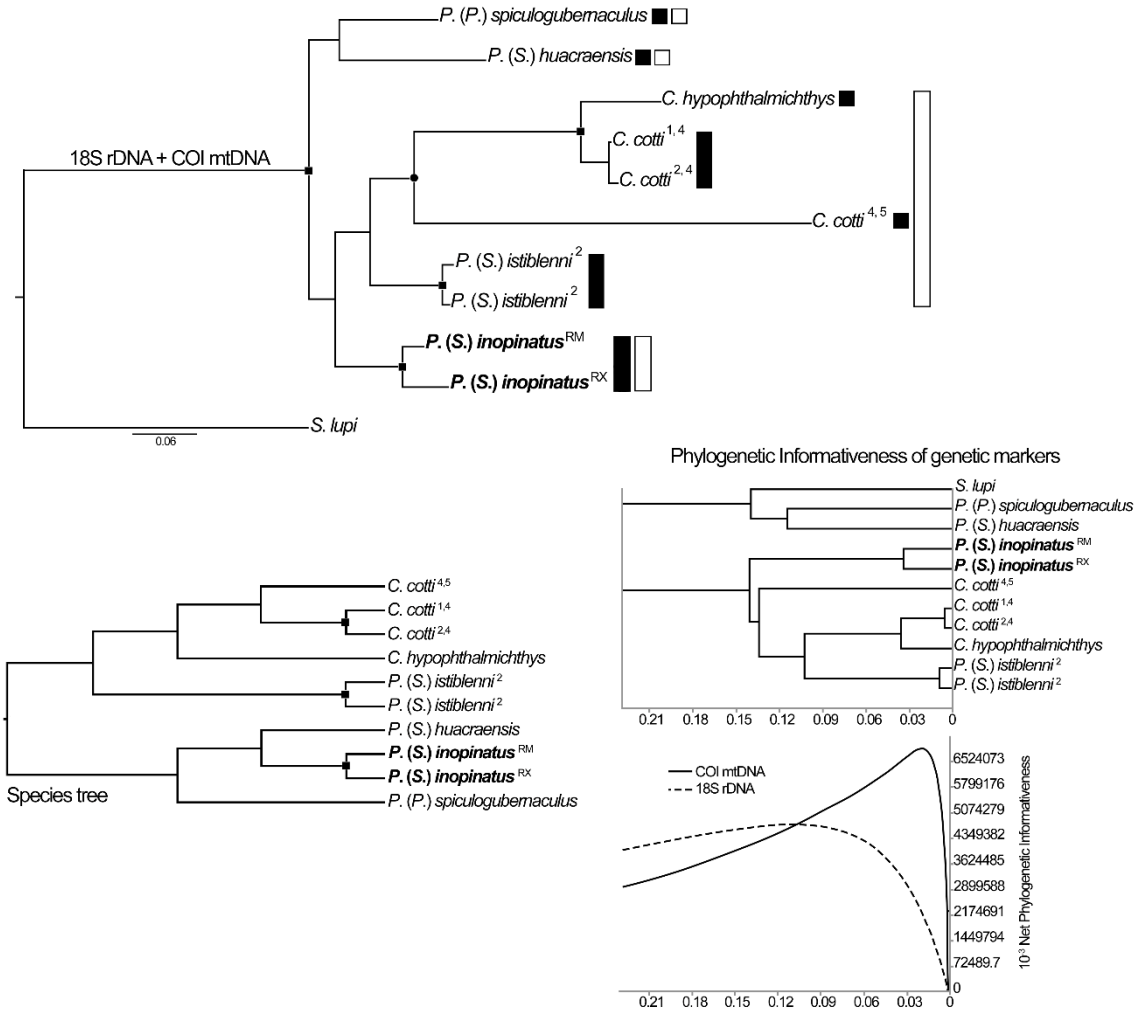

Figure 3.

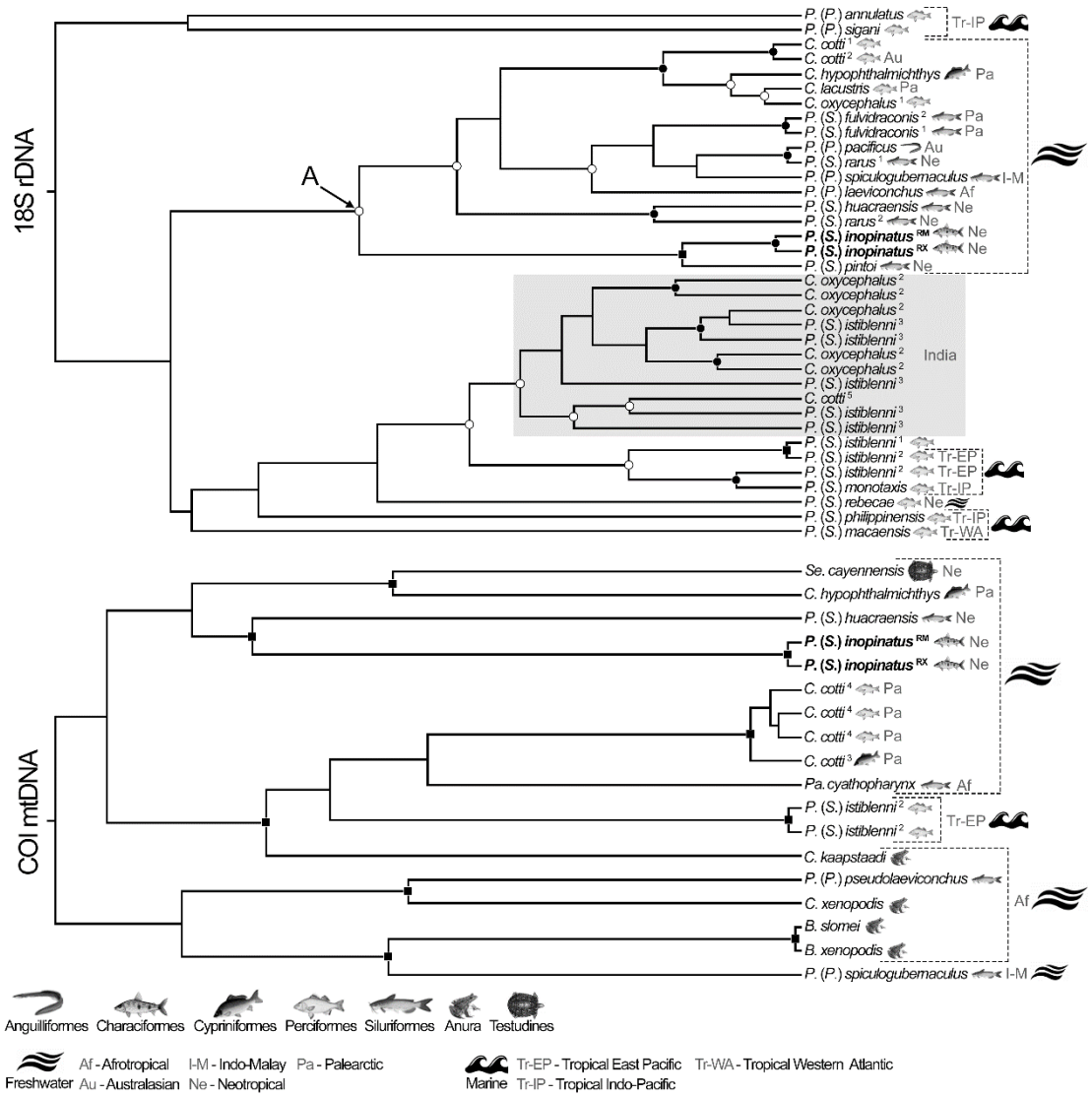

Figure 4.